Eurasian Journal of Physics and Functional Materials

Volume 7 | Number 4

Article 4

Pages: 239 - 248

12-22-2023

Characterization and luminescence dynamics of MgF2:W ceramics

A.V. Strelkova
L.N. Gumilyov Eurasian National University ,Kazakhstan

V. M. Lisitsyn
National Research Tomsk Polytechnic University ,Russian Federation

L. A. Lisitsyna
Tomsk State University of Architecture and Building ,Russian Federation

T.A. Koketai
E.A. Buketova Karaganda University ,Kazakhstan

D. A. Mussakhanov
L.N. Gumilyov Eurasian National University ,Kazakhstan

See next page for additional authors

Recommended Citation

Strelkova, A.V.; Lisitsyn, V. M.; Lisitsyna, L. A.; Koketai, T.A.; Mussakhanov, D. A.; Karipbayev, Zh.T.; and Zhunusbekov, A. M. (2023) "Characterization and luminescence dynamics of MgF2:W ceramics," *Eurasian Journal of Physics and Functional Materials*: Vol. 7: No. 4, Article 4.
DOI: https://doi.org/10.32523/ejpfm.2023070404

Characterization and luminescence dynamics of MgF2:W ceramics

Authors

A.V. Strelkova, V. M. Lisitsyn, L. A. Lisitsyna, T.A. Koketai, D. A. Mussakhanov, Zh.T. Karipbayev, and A. M. Zhunusbekov

Eurasian Journal of Physics and Functional Materials

2023, 7(4), 239-248

Characterization and luminescence dynamics of MgF_2:W ceramics

A.V. Strelkova[1], V.M. Lisitsyn[2], L.A. Lisitsyna[3], T.A. Koketai[4], D.A. Mussakhanov[1], Zh.T. Karipbayev[*,1], A.M. Zhunusbekov[*,1]

[1]L.N. Gumilyov Eurasian National University, Astana, Kazakhstan,

[2]National Research Tomsk Polytechnic University, Tomsk, Russia,

[3]Tomsk State University of Architecture and Building, Tomsk, Russia

[4]E.A. Buketova Karaganda University, Karaganda, Kazakhstan

E-mail: karipbayev_zht_1@enu.kz, zhunusbekov_am@enu.kz

DOI: **10.32523/ejpfm.2023070404**
Received: 13.11.2023 - after revision

This study delves into the synthesis and characterization of luminescent ceramics based on tungsten-activated magnesium fluoride (MgF_2) complemented with varying concentrations of lithium hydroxide (LiOH). Utilizing a distinctive sintering process conducted in an open-air milieu under robust radiation conditions, we successfully synthesized a series of tungsten-activated ceramics. Study revealed that the resultant ceramics prominently display luminescent properties, which can be excited by UV radiation in the spectrum of 200-300 nm, as well as by high-energy electron fluxes. The spectral characteristics of these ceramics, in terms of band position, half-width, and excitation spectra, are strikingly analogous to those observed in LiF crystals activated by tungsten and titanium ions. This observation led to the conclusion that luminescent centers, similar to those in LiF crystals, are formed during the ceramic synthesis.

Keywords: alkaline earth metal fluorides; magnesium fluoride; tungsten; radiation synthesis; luminescence; photoluminescence; kinetic decay

1. Introduction

Optical ceramics have emerged as promising materials for use in applications such as scintillators and phosphors [1–9]. One of the distinguishing characteristics of ceramics is their isotropic properties, meaning they exhibit identical values when measured in different directions. This property allows ceramics to be

crafted into a variety of shapes, thus providing greater flexibility in design and manufacturing. This versatility gives them an edge over traditionally employed monocrystalline materials [10–19].

A material that has garnered significant attention in this domain is optical ceramics based on MgF_2. Just as LiF-based crystals [20–23] have shown potential, MgF_2-based ceramics also hold promise for applications in dosimetric, scintillation materials, and phosphors. A noteworthy advantage of ceramics (or monocrystals) derived from magnesium fluoride is their high melting point. This attribute not only attests to their robustness but also means that products made from it exhibit a high degree of thermal stability.

To enhance the properties of LiF crystals, polyvalent metal ions are often introduced. This is achieved by incorporating metal oxides, such as tungsten, titanium, uranium, and iron, during the growth process. The logic that applies to LiF crystals can be extended to MgF_2 ceramics. To successfully introduce these polyvalent ion activators, the synthesis of magnesium fluoride ceramics must occur in an ambient atmosphere. The reason being, these ions can form volatile compounds with fluorine, which can be problematic. In a vacuum, these potentially volatile compounds are evacuated from the melt, preventing their intended beneficial effects.

Addressing this challenge requires the introduction of co-activators like OH and O ions. These co-activators play a dual role. Firstly, they prevent the formation of volatile compounds between the activator and fluorine. Secondly, they facilitate the integration of activator ions into the ceramic lattice. This process helps in compensating for differences in size and charges compared to the native cations in the material.

A novel approach proposed for synthesizing MgF_2 ceramics in an air atmosphere is the utilization of a powerful electron beam as a heat source, which can be released directly into the environment.

In this study, we delve into the luminescence properties of MgF_2 ceramics activated by tungsten ions. These ceramics were synthesized in an ambient environment, where a powerfull electron beam served as the primary heating mechanism. We aim to elucidate the effects of this unique synthesis method on the optical and structural properties of the resultant ceramics.

2. Ceramic Synthesis

Ceramic samples were prepared using a powerful electron beam as a heat source. To the base mixture of MgF_2 powder, tungsten oxide (WO_3) and lithium hydroxide (LiOH) were added, with weight concentrations ranging from 0.5% to 3%. The blend, with varied compositions, was then poured into conical depressions, each 1 cm in diameter, situated on a solid copper crucible. This crucible was subjected to the electron beam, brought out of a vacuum into an atmosphere at ambient pressure through a differential vacuum pumping system. The electron stream, powered with an energy of 1.4 MeV from the ELV-6 accelerator, was guided along the assembly at a rate of 1 cm/sec. With a cross-section of 0.5

cm^2 at the crucible's surface, the electron beam, within a second, melted the mixture. Once the beam action ceased, the molten mix rapidly solidified, yielding a ceramic sample with the designated additive ratios.

Synthesizing materials under a robust stream of high-energy electrons substantially differs from conventional thermal-field synthesis. Given the employed irradiation conditions, the mixture absorbs energy at a rate of 6×10^{23} eV/cm^3, resulting in approximately 6×10^{22} cm^3 of electronic excitations (ionizations, electron-hole pairs). Hence, the ceramic formations emerge from a highly ionized assembly of the mixture elements, similar to a plasma-like state. This scenario allows for the formation of ceramic from various combinations of atoms and ions and intermixing of the initial powders. Since magnesium and fluorine are predominant in the mixture, the most likely outcome is the formation of a magnesium fluoride crystalline phase interspersed with tungsten, oxygen, and hydrogen ions. Conversely, thermal-field synthesis leaves the electronic subsystem unexcited.

The resulting samples appeared as dark gray plates, 6–8 mm in diameter and 2–4 mm in thickness. The treated side of these samples showcased a melted material appearance.

Post-synthesis, these specimens underwent annealing. The annealing process was executed in a NABERTHERM furnace in an open-air environment. Samples were steadily heated for 60 minutes to reach 1000 °C, where they remained for 7 hours. After this, the samples were allowed to cool gradually.

The annealing transformed these ceramic samples. Their color shifted from gray to a bright white. A closer examination revealed that this color change was predominantly near the surface, within a depth of approximately 0.5–0.7 mm. SEM images and elemental composition of samples MgF_2 +3.0% WO_3 +3% LiOH, captured using the Quanta 3D 200i scanning electron microscope at 15 KeV, are presented in Figure 1. The surface of the synthesized sample bore the appearance of solidified molten material interspersed with particles of the unmelted mixture. The samples primarily consisted of Mg, F, and W elements. Post-annealing, the sample surface seemed like coalesced particles with elongated oval shapes, about 5–7 μm in length and 2–3 μm in diameter. The annealed samples predominantly contained Mg, O, and W. Similar surface transformations were observed in samples with different initial mixture compositions.

Note that the above measurements show the composition only near the surface of the samples, particles at a depth of about 10 nm.

There's no evident correlation between the change in morphology and the degree of doping. The differences might be explained by variations in the structural and phase composition from one sample to another due to differences in synthesis conditions. The ceramic synthesis – rapid heating by radiation, followed by cooling – occurs under poorly controlled conditions. For instance, heat dissipation from the central part of the copper crucible takes longer than from the edges. The melting zone's temperature was adequate to melt the charge over the entire surface, but it was not uniform across the surface. After annealing, the sample surfaces remained unchanged, but there was a significant reduction in the number of small particles on the surface.

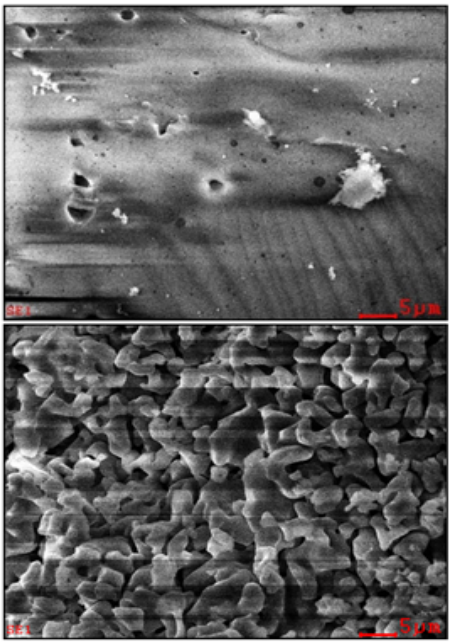

1

Element	At%
O	33.41
Mg	64.78
W	1.81

2

Element	At%
F	54.64
Mg	44.23
W	1.13

Figure 1. SEM images and elemental analysis tables of the $MgF_2 + 3.0\%\ WO_3 + 3\%$ LiOH ceramic surface before (1) and after (2) thermal treatment.

3. Luminescence of ceramics

Studies were conducted on the excitation and luminescence spectra of synthesized MgF_2 ceramic samples containing WO_3 in the charge at weight concentrations of 0.5, 1, and 3%, and $MgF_2 + 3\%\ WO_3$ with weight concentrations of LiOH at 0.5, 1, and 3%. Measurements were carried out using the Solar CM2205 spectrophotometer.

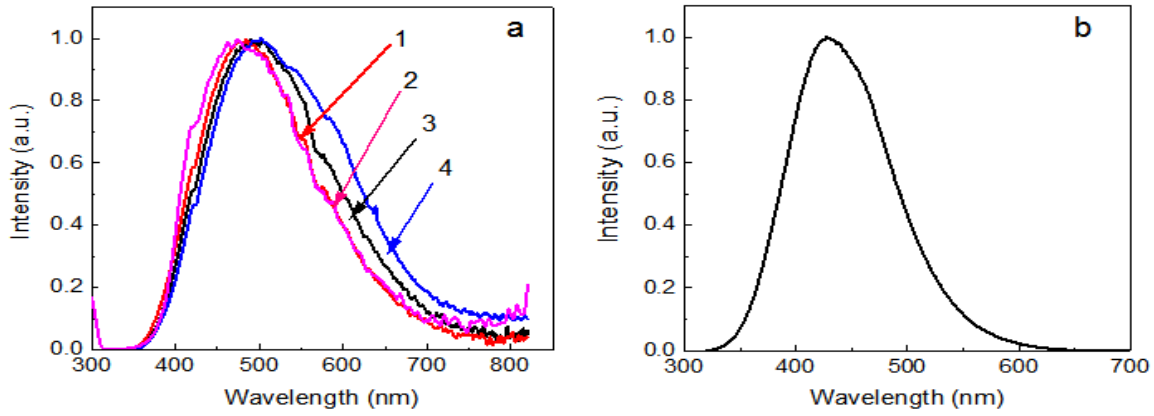

Figure 2. Luminescence spectra of synthesized exited at 250 nm ceramic samples differing in initial charge composition: a) 1 – $MgF_2 + 0.5\%\ WO_3 + 3.0\%$ LiOH; 2 – $MgF_2 + 3.0\%\ WO_3 + 3\%$ LiOH; 3 – $MgF_2 + 0.5\%\ WO_3$; 4 – $MgF_2 + 3.0\%\ WO_3$; and b) LiF:W crystal.

Ceramics synthesized from specially purified magnesium fluoride raw materials, prepared for the growth of ultra-pure MgF_2 crystals, practically do not luminesce when excited with radiation in the range of 200–500 nm. The results of the study of luminescence spectra of ceramic samples synthesized from a charge with additives of activators before annealing are shown in Figure 2.

Upon excitation with radiation in the range of 200–300 nm, luminescence is observed in the 340–650 nm range. The luminescence spectra appear as a band with a well-defined emission maximum in the 480 nm range. The position and shape of the luminescence bands weakly depend on the concentration of the introduced impurities. The characteristics of the luminescence bands of the samples are given in Table 1.

Figure 2b shows the luminescence spectrum of a tungsten-activated LiF:W crystal (grown by the Kyropoulos method in air at ISMA NAS of Ukraine (Kharkov). The luminescence spectrum appears as a single band with a maximum at 450 nm and a half-width of 0.7 eV. It can be seen that the spectral characteristics of the luminescence in the LiF:W crystal and MgF_2:W ceramics are close. This indicates a similarity in the luminescence centers in these materials. Some quantitative difference in half-width and luminescence maximum are associated with differences in crystal lattice parameters is explained by the difference in structure, primarily lattice parameters: a=4.8322, c=3.3099 for MgF_2 ceramic, and a=4.01989 for LiF:W crystal [24].

The excitation spectrum of luminescence for samples that have not been annealed has three distinct regions (Figure 3). Luminescence increases with decreasing excitation wavelength from 300 to 270 nm, then remains almost unchanged up to 230 nm and sharply rises to 200 nm. The nature of the excitation spectrum does not depend on the concentration of the introduced impurity.

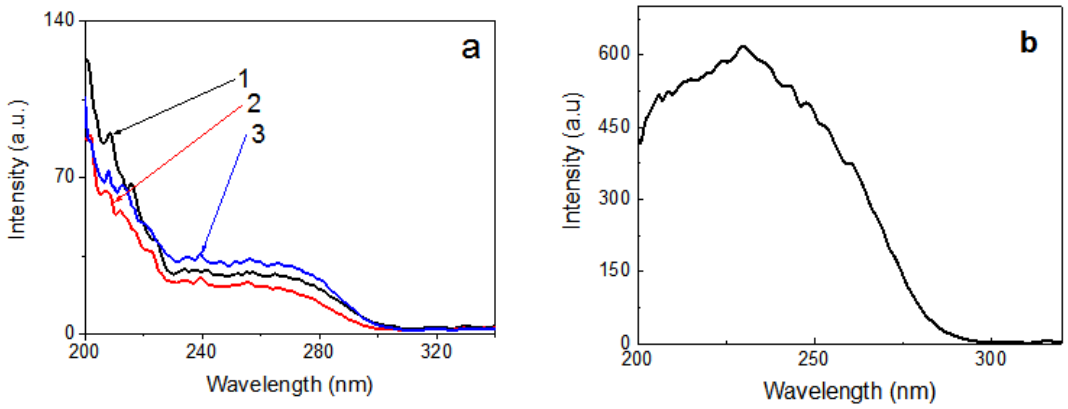

Figure 3. Excitation spectra of luminescence of ceramic samples differing in the composition of the initial batch: a: 1 – MgF_2 + 3% WO_3, 2 – MgF_2 + 0.5% WO_3 and +3% LiOH, 3 – MgF_2 + 3% WO_2 + 3% LiOH and b: of the LiF:W crystal.

Figure 3b shows the excitation spectrum of luminescence of the tungsten-activated LiF:W crystal. The excitation spectrum is complex and continuous, falling within the same range as in MgF_2:W. This also indicates the similarity of luminescence centers in these materials.

The results of the luminescence spectrum study of annealed ceramic samples are shown in Figure 4. Luminescence, when excited by radiation in the 250 nm range, is observed in the same spectral region as in the unannealed samples. Table 1 presents the values of the position and half-width of the luminescence bands of the samples.

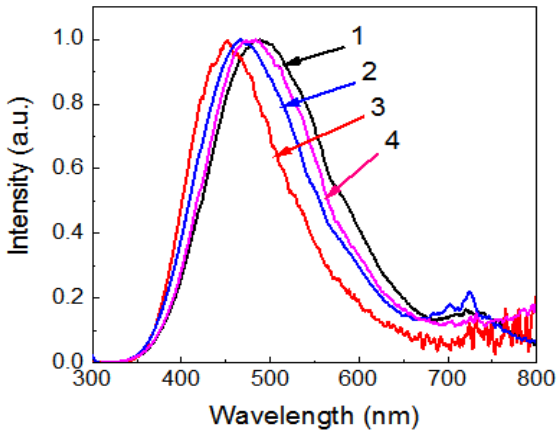

Figure 4. Luminescence spectra of annealed samples excited at 250 nm 1 – $MgF_2 + 0.5$ W (11), 2 – $MgF_2 + 0.5$ W+3OH (51), 3 – $MgF_2 + 3$ W (23), 4 – $MgF_2 + 3$ W+3OH (52) when.

Table 1.
Characteristics of the photoluminescence spectra of ceramic samples before and after annealing when excited at 250 nm.

Sample	Before annealing		After annealing	
	λ_{max}	ΔE, eV	λ_{max}	ΔE, eV
MgF_2 + 3.0% WO_3	485	0.8	450	0.74
MgF_2 + 0.5% WO_3 + 3.0% LiOH	475	0.8	475	0.8
MgF_2+ 3.0% WO_3 + 3% LiOH	475	0.8	485	0.8

The emission centers comprise tungsten ions and oxygen ions. The authors' earlier assumption that admixture complexes containing polyvalent ions, which function as nano-sized excitation sinks, is supported by the comparable light yields in these crystals and the significant variation in luminescence center concentrations between them. These excitation sinks have the potential to capture electronic excitations with a cross-section approximately two orders of magnitude larger than that of point defects. The presence of these excitation sinks in the vicinity of impurity complexes containing luminescence centers contributes significantly to the high light yield observed in phosphors based on LiF crystals with polyvalent metal oxides [25–27].

When comparing the characteristics of the luminescence spectra of ceramic samples before and after annealing, it's evident that in the range of $300 \div 650$ nm, they are largely similar. The peak positions of the bands lie within the $450 \div 485$ nm range. No connection between the position of the bands and the sample composition is observed. Apparently, the luminescence is attributed to the same luminescent centers, and any shift is explained by variations in the structure in the immediate vicinity of the luminescent centers. It should be emphasized that the luminescence spectra of ceramic samples when excited by radiation in the $300 \div 240$ nm range are similar, even though the surface morphology and the composition near the surface differ significantly. This can be explained by the

fact that the elemental composition was measured at the surface, over a thickness of about 10 nm. Therefore, luminescence is excited throughout the volume.

A significant difference in the luminescence spectra of samples after annealing is the appearance of an additional band in the 720 nm range when excited by radiation with $\lambda = 200 \div 230$ nm. An example of such luminescence spectra is shown in Figure 5.

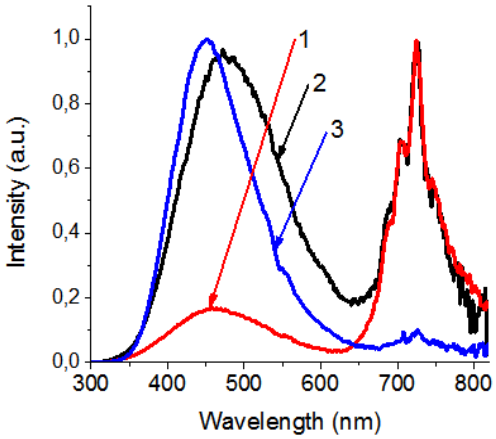

Figure 5. Luminescence spectra of annealed samples when excited at 200 nm. 1 – $MgF_2 + 0.5\%\ WO_3$ and +3.0% LiOH; 2 – $MgF_2 + 3.0\%\ WO_3 + 3\%$ LiOH; 3 – $MgF_2 + 3.0\%\ WO_3$.

As shown in Figure 5, the band at $\sim$720 nm is intense in samples with a high content of OH. The band at $\sim$480 nm remains dominant in samples with a high content of tungsten.

Figure 6 presents the results of a study on the excitation spectra of ceramic samples after annealing. The excitation spectra of the MgF_2 + WO_3 samples are mostly similar to those measured in ceramic samples before annealing. Luminescence in them is excited by radiation in the range from 310 to 200 nm. Luminescence with a band maximum at 720 nm is excited only by radiation in the region of 200 nm.

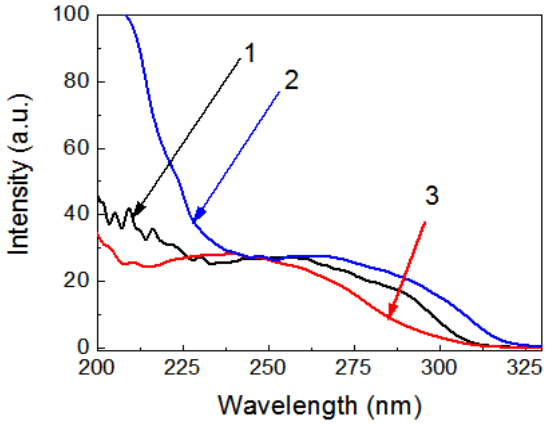

Figure 6. Luminescence excitation spectra of annealed ceramic samples with different initial batch compositions: 1 – $MgF_2 + 0.5\%\ WO_3$; 2 – $MgF_2 + 3.0\%\ WO_3 + 3\%$ LiOH; 3 – $MgF_2 + 3.0\%\ WO_3$.

Spectral characteristics of luminescence of synthesized MgF_2 ceramic samples before and after annealing were studied when excited by pulse electron beams

with an average energy of 250 KeV. It is shown that the spectral characteristics of ceramic samples before and after annealing are similar to those measured during photoexcitation. The general spectral characteristics of ceramic samples are presented in Table 1. Some differences are due to the influence of the magnesium oxide layer in the annealed sample.

Figure 7 and Table 2 show the results of the study of the luminescence decay kinetics of samples before and after annealing. The decay kinetics of luminescence after excitation by an electron beam pulse is multi-stage. At least three components are distinguished: nanosecond, microsecond, and a component with a characteristic time in the range of $18 \div 33$ μs. Luminescence kinetics is weakly dependent on the sample's history, composition, and annealing. This indicates that the luminescent centers are identical in all the studied samples.

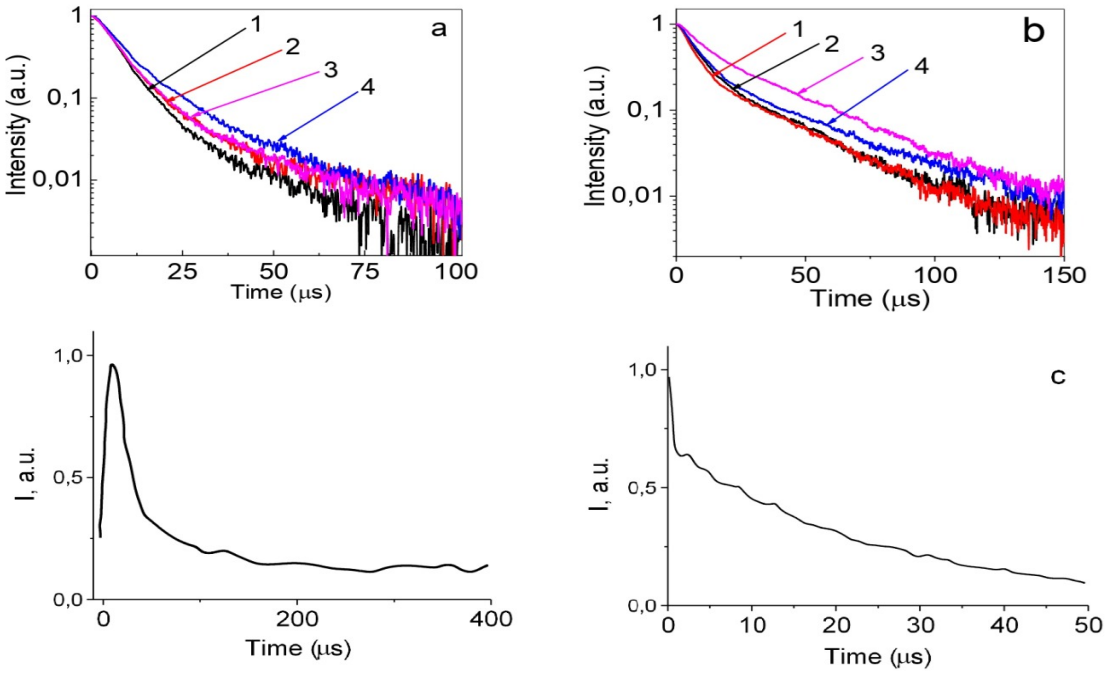

Figure 7. Kinetic decay curves of luminescence of ceramic samples before (a) and after (b) annealing. 1 – $MgF_2 + 3.0\%\ WO_3$; 2 – $MgF_2 + 0.5\%\ WO_3$; 3 – $MgF_2 + 3.0\%\ WO_3 + 3\%$ LiOH; 4 – $MgF_2 + 0.5\%\ WO_3 + 3\%$ LiOH and crystals: (c) crystal of LiF:W.

Table 2.
Kinetic decay characteristics of samples before and after annealing.

Sample	Before annealing				After annealing			
	A_1	A_2	τ_1, μs	τ_2, μs	A_1	A_2	τ_1, μs	τ_2, μs
MgF_2 + 3.0% WO_3	0.165	0.037	4.2	18.7	0.172	0.03	4.02	23.07
MgF_2 + 0.5% WO_3 + 3.0% LiOH	0.155	0.020	4.46	33.6	0.14	0.026	4.95	25.83
MgF_2+ 3.0% WO_3 + 3% LiOH	0.146	0.032	4.74	21.4	0.13	0.029	5.36	24.18

Figure 7c illustrates the kinetic decay curves of luminescence in LiF:W crystals, triggered by a nanosecond-duration electron flux pulse. The decay kinetics distinctly exhibit three luminescence decay components. As inferred from the

results depicted in Figure 7, the kinetic decay curves of the ceramic samples can be described by a combination of components with characteristic decay times similar to those measured in LiF:W crystals.

Conclusion

Samples of ceramics based on tungsten-activated magnesium fluoride and containing varying additions of lithium hydroxide (LiOH) have been synthesized. The sintering of the oxidebased mixture was carried out in an open-air environment under the influence of a powerful radiation field. Through detailed examination, it has been established that the resulting tungsten-activated ceramic exhibits luminescent properties. This luminescence can be excited by UV radiation in the range of 200–300 nm and by high-energy electron streams.

The spectral characteristics of the ceramic luminescence, including the position and half-width of the bands, as well as the excitation spectra of photoluminescence, closely resemble those known for crystals of LiF doped bytungsten ions. This similarity suggests that during the synthesis of the tungsten-activated MgF_2 ceramic, luminescent centers were formed, structurally analogous to those identified in LiF crystals [26–28].

It is plausible to hypothesize that the synthesis of activated MgF_2 ceramics results in the formation of nanodefects. These defects are potentially similar to those described in references [29–32] and are capable of efficiently absorbing excitation energy and transferring it to luminescent centers.

Acknowledgments

This research has been funded by the Science Committee of the Ministry of Education and Science of the Republic of Kazakhstan (Grant No. AP14871114) and by the Russian Science Foundation of the Russian Federation (Grant No. 23-73-00108).

References

[1] A. Ikesue et al., Annual Review of Materials Research **36** (2006) 397–429. [*CrossRef*]
[2] T.T. Basiev, Izv. Ros. Acad. Sciences. Ser. Chem. **5** (2008) 863–872. (In Russian)
[3] V.I. Solomonov et al., Optics and Spectroscopy **117** (2014) 908–913. [*CrossRef*]
[4] V.V. Osipov et al., Optical Materials **71** (2017) 98–102. [*CrossRef*]
[5] O.V. Palashov et al., Quantum Electronics **37** (2007) 27. [*CrossRef*]
[6] O.V. Palashov et al., Quantum Electronics **39** (2009) 943–947. [*CrossRef*]
[7] T.T Basiev et al., Physics-Uspekhi **54** (2011) 1262. [*CrossRef*]
[8] Jasbinder Sanghera et al., Materials **5**(2) (2012) 258–277. [*CrossRef*]
[9] V.A. Maslov et al., Inorg. Mater. Appl. Res. **3** (2012) 113–119. [*CrossRef*]

[10] B. Lu et al., Journal of the American Ceramic Society **98** (2015) 2480–2487. [*CrossRef*]
[11] M. Cao et al., Optical Materials **76** (2018) 323–328. [*CrossRef*]
[12] M. Cao et al., Ceramics International **43** (2017) 2165–2169. [*CrossRef*]
[13] Z.M. Seeley et al., Optical Materials **35** (2012) 74–78. [*CrossRef*]
[14] V.M. Lisitsyn et al., Nuclear Instruments and Methods in Physics Research Section B: Beam Interactions with Materials and Atoms **374** (2016) 24–28. [*CrossRef*]
[15] E.A. Kotomin et al., Journal of Physics: Condensed Matter **4** (1992) 5901-5910. [*CrossRef*]
[16] V.N. Kuzovkov et al., Nuclear Instruments and Methods in Physics Research Section B: Beam Interactions with Materials and Atoms **435** (2018) 79–82. [*CrossRef*]
[17] A.I. Popov et al., Nuclear Instruments and Methods in Physics Research Section B: Beam Interactions with Materials and Atoms **480** (2020) 16–21. [*CrossRef*]
[18] A.B. Usseinov et al., Nuclear Instruments and Methods in Physics Research Section B: Beam Interactions with Materials and Atoms **470** (2020) 10–14. [*CrossRef*]
[19] E.A. Kotomin et al., Radiation Effects and Defects in Solids **155** (2001) 113–125. [*CrossRef*]
[20] V. Pankratov et al., Journal of Luminescence **94-95** (2001) 427–432. [*CrossRef*]
[21] M. Nikl et al., Physica Status Solidi (b) **245** (2008) 1701–1722 [*CrossRef*]
[22] L.A. Lisitsyna et al., Optics and Spectroscopy **105** (2008) 531–537. [*CrossRef*]
[23] L.A. Lisitsyna et al., Optics and Spectroscopy **112** (2012) 175–181. [*CrossRef*]
[24] V. Lisitsyn et al., Nuclear Instruments and Methods in Physics Research Section B: Beam Interactions with Materials and Atoms **435** (2018) 263–267. [*CrossRef*]
[25] L.A. Lisitsyna et al., Russian Physics Journal **60** (2017) 593–599. [*CrossRef*]
[26] L.A. Lisitsyna et al., Inorganic Materials **47** (2011) 531–534. [*CrossRef*]
[27] L.A. Lisitsyna et al., Physics of the Solid State **55** (2013) 2297–2303. [*CrossRef*]
[28] L.A. Lisitsyna et al., Journal of Physics: Conference Series **830** 0012156 (2017) 012156. [*CrossRef*]
[29] V.M. Lisitsyn et al., Journal of Luminescence **153** (2014) 130–135. [*CrossRef*]
[30] V. Lisitsyn et al., IOP Conf. Series: Materials Science and Engineering **81** (2015) 012020. [*CrossRef*]
[31] V. Lisitsyn et al., IOP Conference Series: Materials Science and Engineering **168** (2017) 012086. [*CrossRef*]
[32] T.A. Koketai et al., Eurasian Journal of Physics and Functional Materials **7**(1) (2023) 45–51. [*CrossRef*]